Chapter 5

DETERMINATION OF Pb CONCENTRATION USING XRF METHOD

Introduction

There are few methods available, which can be used to detect the presence of Pb in a material, namely Sodium Sulfide Testing, Atomic Absorption Spectrophotometry (AAS) and X-ray Fluorescence Analyzer (XRF). Sodium sulfide solution can be used to detect the presence of Pb in liquid solution by applying some of it to the solution. It reacts with the Pb to yield lead sulfide, which appears black or gray in color. However, this method is difficult to test materials, which are dark in color. AAS is used to analyze lead by atomizing the sample into a flame, furnace or by other atomization techniques. The instrument will measure the amount of lead that is vaporized. XRF is a non-destructive method whereby the raw materials may be analyzed qualitatively, without any preparation by using the radioactive source to excite lead atoms in the sample. As they return to normal state, the atoms emit X-rays that are characteristics of lead.

In this study the XRF technique is used to measure the lead concentration. The determination of different concentrations of lead in solution form had been carried out. After the calibration, the system was set as described in chapter 4, and remained unchanged throughout the whole experiment. The experimental results are tabulated and discussed. The statistical average mean of differentiation is applied to

maximize the spectral information and thus used as the standard calibration for assessing the final determination of the lead concentration in human teeth.

Semi-empirical theory is used to perform the calculation of counts detected as a comparison to the real experimental results, which is presented in the last part of this chapter.

5.1 Results and Discussion

This study was carried out with the detection of Pb spectrum in order to identify the position of the K-lines in MCA. The measurement of background effect had to be determined first to eliminate the contamination from the surrounding equipment or from the ultra-pure water itself. Besides, these background measurements were vital also for comparison with each respective Pb concentration presence using the method of average mean of difference.

5.1.1 Comparison the Measurement of Background and Pure Pb Spectrum

Figure 5.1 shows one of the background spectrums prior to measuring the K-lines of Pb. Triple ultra-pure water, without any contamination of Pb was used in this measurement. Here, the dominant peaks of 72.8 keV and 75 keV due to Pb X-ray fluorescence is not observed in this graph.

Figure 5.2 shows the Pb's spectrum of XRF with high concentration of lead in which 3.2 g of lead powder was added into the 10 ml of triple ultra pure water. Clear and obvious peaks due to the XRF of Pb K-lines are observed and marked in the graph. The respective channels of the peaks have been identified and will be used for further measurements of lead K-lines in various Pb concentrations.

All the figures present the spectrum in the range of channels within 140 to 180 with the purpose to eliminate the domination of Tc-99m spectrum, which appears at channel 300 as shown in figure 5.2. The total count of Tc-99m is much higher if compared with others, thus, the Pb K-lines spectrum will not be seen clearly if the whole spectrum was presented, especially for low Pb concentrations. Therefore, with the elimination of Tc-99m spectrum, the peaks of Pb K-lines would appear clearly in that range.

All these measurements had been made over a counting live time of 400 s.

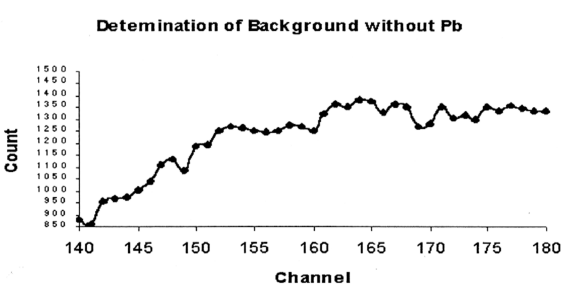

Figure 5.1: The Determination of Background Spectrum (Ultra-pure Water & Tc-99m)

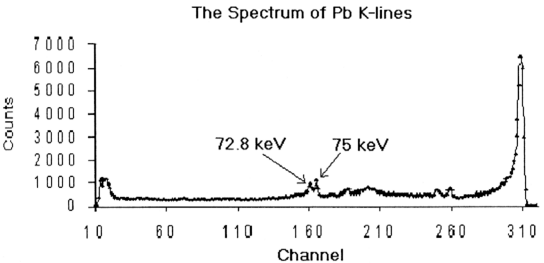

Figure 5.2: The Pb Spectrum: Pb Powder (3.2 ± 0.1 g) in 10 ml Ultra Pure Water

5.1.2 Spectrum of Pb XRF K-lines from the Concentration of 1000 ppm to 100 ppm

Figure 5.3 (a) shows the spectrum of Pb with the concentration of 1000 ppm. The peaks appear in the channels of 160-163 and 164-169 are clear compared to the background spectrum (figure 5.1). The energy resolutions of the peaks of 72.8keV and 75 keV are found to be corresponding at 277 eV and 315 eV respectively.

Figure 5.3 (b) shows the K-line peaks of Pb with the concentration of 900 ppm and the identified range of channels are still observable. However, the resolution energy, which correspond to the respective peaks have increased to 289 eV and 327 eV. The heights of the peaks are also slightly flattened as compared with the figure 5.3 (a). From figure 5.3 (c), the spectrum of Pb (800 ppm) K-lines is still observable. However, the energy resolution of the peaks has increased if compared

with figures 5.3 (a) and 5.3 (b). The energy resolution for 72.8 keV and 75 keV are 295 eV and 339 eV respectively. The peak of $K_{\alpha 1}$ (75 keV) has slightly shifted to the right and flattened as compared with the previous figures. This could be caused by the less sensitivity of the XR-100T detector in detecting the Pb concentration lower than 900 ppm.

From figures 5.3 (d) to 5.3 (g), the concentration of Pb had been reduced to 600 ppm, 400 ppm, 200 ppm and 100 ppm respectively, and the peaks of K-lines are not clearly observed as shown in the figures 5.3 (a), 5.3 (b) and 5.3 (c). The resolution of the detector to differentiate the peak of 72.8 keV and 75 keV becomes weak as the concentration decreases. Figure 5.3 (d) (Pb-600 ppm) and 5.3 (e) (Pb-400 ppm) show only one peak situated in the channel number between 163 to 168, with the corresponding energy at 74.5 keV and energy resolution of 385 eV. The sensitivity of the detector decreases, as the concentration of Pb reached 800 ppm.

In fact the detector system is not able to identify the K-lines for Pb concentrations below 400 ppm. As shown in figure 5.3 (f) (Pb-200 ppm) and 5.3 (g) (Pb-100 ppm), the peaks of K-lines are unidentified and cannot be significantly differentiated from the background spectrum.

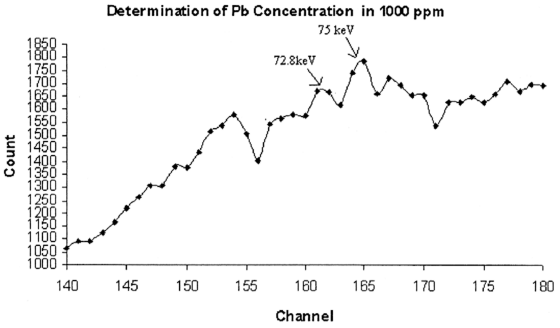
Determination of Pb Concentration in 1000 ppm
75 keV
72.8keV
Count
Channel

(a)

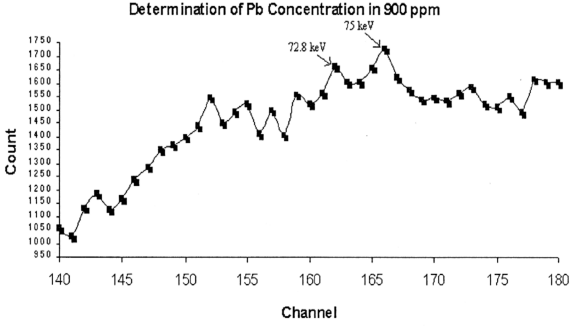
Determination of Pb Concentration in 900 ppm
75 keV
72.8 keV
Count
Channel

(b)

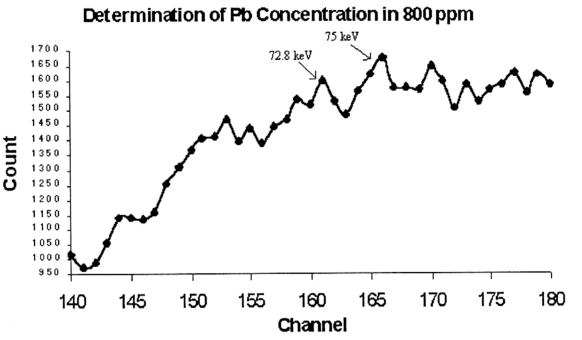
Determination of Pb Concentration in 800 ppm
75 keV
72.8 keV
Count
1700
1650
1600
1550
1500
1450
1400
1350
1300
1250
1200
1150
1100
1050
1000
950
140
145
150
155
160
165
170
175
180
Channel

(c)

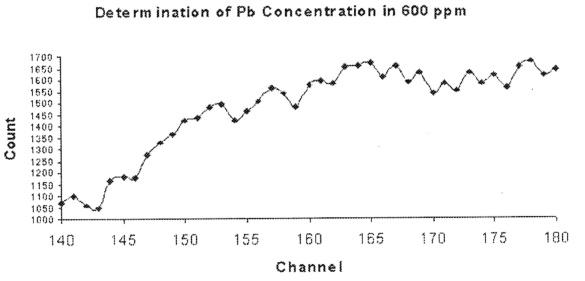
Determination of Pb Concentration in 600 ppm
Count
1700
1650
1600
1550
1500
1450
1400
1350
1300
1250
1200
1150
1100
1050
1000
140
145
150
155
160
165
170
175
180
Channel

(d)

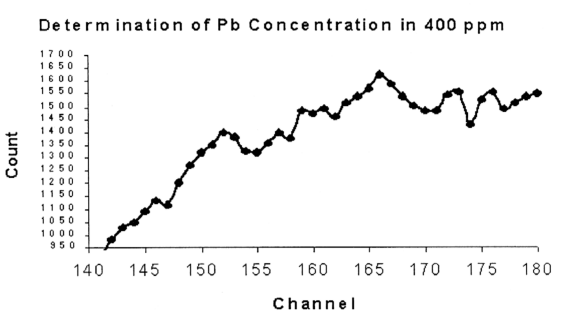
Determination of Pb Concentration in 400 ppm
Count
1700
1650
1600
1550
1500
1450
1400
1350
1300
1250
1200
1150
1100
1050
1000
950
140
145
150
155
160
165
170
175
180
Channel

(e)

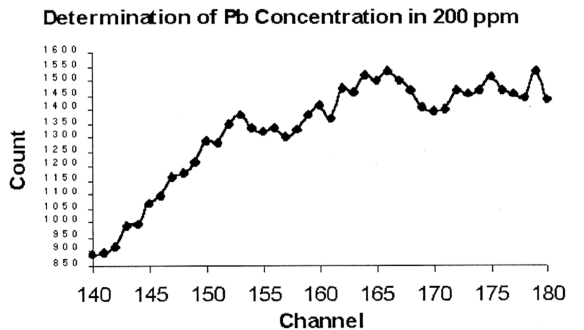
Determination of Pb Concentration in 200 ppm
Count
1600
1550
1500
1450
1400
1350
1300
1250
1200
1150
1100
1050
1000
950
900
850
140
145
150
155
160
165
170
175
180
Channel

(f)

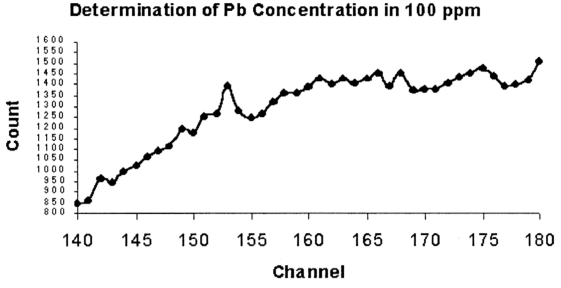

(g)

Figure 5.3: The Spectrum of Pb K_α with the Concentration of (a) 1000ppm (b) 900ppm (c) 800ppm (d) 600ppm (e) 400ppm (f) 200ppm and (g) 100ppm

5.1.3 Average Mean of Difference—Used to Maximize the Spectral Information

In order to maximize the spectral information and to set-up the standard calibration for the final determination of the lead concentration in the human teeth, the average mean of difference is applied. The average mean of difference is based on the normalization over time integrated area under each spectrum of concentration to unity.

The total counts of $K_{\alpha 1}$ and $K_{\alpha 2}$ are determined and then normalized with the total counts of Tc-99m; whose energy is 140.5 keV. Normalizing the reading avoids the correction for the decay counts of the source. Then a comparison is made to the normalized background spectrum.

Each concentration of Pb is normalized and compared with the respective background measurements.

Table 5.1: Normalized Total Counts of $K_{\alpha 1}$ and $K_{\alpha 2}$ for Each Concentration of Pb

Concentration (ppm)	Mean	Error	Percent
1000	0.149	0.002	1.11
900	0.162	0.002	1.13
800	0.152	0.002	1.12
600	0.127	0.001	1.12
400	0.126	0.001	1.14
200	0.135	0.002	1.17
100	0.134	0.001	1.49

Table 5.2: Normalized Total Counts of $K_{\alpha 1}$ and $K_{\alpha 2}$ for the Measurement of Background for Each Concentration of Pb

Concentration (ppm)	Mean	Error	Percent
1000	0.138	0.002	1.17
900	0.153	0.002	1.17
800	0.144	0.002	1.16
600	0.120	0.001	1.16
400	0.121	0.001	1.17
200	0.130	0.002	1.19
100	0.125	0.002	1.16

The table 5.3 shows the average mean of difference for each concentration. The average mean of difference for concentration of 1000 ppm is 8.49 ± 2.69 %; the value decreases as the concentration of Pb decreased. For 100 ppm, the average mean of difference is about 1%, which shows no significant difference from the background measurement.

Table 5.3: Average Mean of Difference (AMD) for each different lead concentration

	1000 ppm	900 ppm	800 ppm	600 ppm	400 ppm	200 ppm	100 ppm
AMD in %	8.49 ± 2.69	5.87 ± 2.67	5.64 ± 2.65	5.23 ± 2.64	4.20 ± 2.65	3.57 ± 2.71	1.05 ± 2.68

The standard error of the measurement is determined. The error ranges from 2.6% to 2.7% for all the measurements in which the error could be considered to be constant throughout the whole practical work. However, the percentage error of average mean of difference for each concentration is high as shown at the table 5.4 below. As the concentration of Pb decreases to 100 ppm, the error of the measurement becomes higher. Therefore, this system is not suitable to measure the concentration, which is below 800 ppm of Pb.

Table 5.4: The Error in % Increase Significantly as the Concentration of Pb Decreasing

	1000 ppm	900 ppm	800 ppm	600 ppm	400 ppm	200 ppm	100 ppm
The % of Error	31.7	45.5	46.9	50.4	63.0	75.9	255.0

Figure 5.4 shows a linear relationship between the average mean of differences (%) and the concentration of Pb (ppm). The linear regression equation derived from this experiment is the Average Mean of Difference (%) = 0.0061x (concentration in ppm) + 1.3909, and the regression coefficient of this linear graph is, R = 0.927. Therefore, in view of the inability of the system to significantly identify the peaks of K X-rays of Pb at concentrations below 800 ppm, this linear regression equation is insufficient to produce any good applicable linear concentration result for the lead concentration in human teeth, which is lower than 50 ppm. (P.Bloch et. al., 1976).

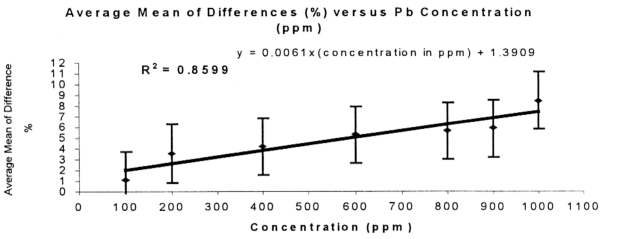

Figure 5.4: Average Mean of Differences in percentage versus the Concentration of Pb in ppm

The major difference between this experiment and earlier work done by D.A. Bradley, Lynn Kissel and R.H.Pratt (1999) is the different excitation sources being used. They used ^{109}Cd, with the energy peak at 88.036 keV. Other researchers, who had performed the same work under active development, employed ^{109}Cd to excite the K x-rays. They were Chettle et al (1991), Webber et al (1992) and Green et al (1992).

Therefore, we can conclude that this experiment set-up is merely functional to detect the K X-rays of Pb for lead concentrations above 800 ppm.

For lower photon energies, photoelectric interactions are much more predominant than Compton (K. Debertin and R.G. Helmer, 1988). Over most of the energy range, the probability of both photoelectric and Compton interactions decreases with the increase of energy. However, the decrease in the photoelectric interactions is much greater; whereby rate change is proportional to $1/E^3$ and E is the energy of photon. In order to enhance the photoelectric interactions, excitation

source with lower photon energies should be used such as Cd-109 with gamma energy of 88.036 keV compared with Tc-99m (140.5 keV). A source with gamma energy just above the binding energy of K shell of lead would have a very large cross section of photoelectric interaction and hence a more sensitive system is required.

5.2 Theoretical Model

To further confirm the experimental results above, a theoretical model has been developed to calculate the total count under the peak of $K_{\alpha 1}$ (75 keV) line of Pb. A comparison of theoretical and experimental value was carried out.

5.2.1 Calculation of the Total Count for the line $K_{\alpha 1}$

In quantitative analysis of XRF spectrometer, it is the secondary spectral-line intensity emitted by the analyte, which is measured. This is also used to determine the analyte concentration.

Table 5.5 (from K.Debertin and R.G.Helmer, 1988) shows the relative emission for K X-rays of Pb and K shell Fluorescence yields:

Z	K_{β} / K_{α}	$K_{\alpha 2} / K_{\alpha 1}$	$K_{\beta 1} / K_{\alpha 1}$	$K_{\beta 2} / K_{\alpha 1}$	ω_k
82	0.280	0.593	0.353	0.102	0.963

Table 5.5: Relative Emission and Fluorescence Yields for Pb

5.2.2 Geometrical Set-up of the Experiment

In order to calculate the counts of Pb K-lines, the exact geometrical set-up of the experiment has to be known. Figure 5.5 shows the dimensions of the experimental set-up.

The target sample is positioned orthogonal via the detector as well as the radiation excitation source. The incident angle of the primary beam is ϕ, and the take off angle of the secondary beam is ψ. Both angles are situated at $\pi/2$ respectively tangent to the target and detector.

It is assumed a single wavelength λ_{pri} (E=140.5 keV) of Tc-99m having the intensity of I_o (activity = 40.3 mCi) is the incident primary beam.

The analyte, is the standard lead solution with a known concentration filled in the thin transparency plastic bag. It was placed 25 cm from the detector.

The size of the detector is (3x3) mm^2 with the thickness of 2 mm. The detection efficiency is 100% as the energy to be detected is below 100 keV as shown in figure 4.4.

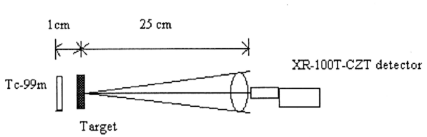

Figure 5.5: The Schematic of Geometrical Set-up of the Experiment

Table 5.6: Summary of the Value for each item in the equation:

ω_A (fluorescence yield of Pb)	0.963
g_k (Relative intensity of the analyte Pb line in its series)	0.7936
$(r_{Pb} - 1) / r_{Pb}$ (Absorption edge jump ratio)	0.75 (E.P. Bertin, 1978)
$d\Omega/4\pi$ (fraction of analyte-line photons emitted toward source collimator)	8.913×10^{-6}
$A = \sin\phi / \sin\psi$ (Geometric factor)	1
C_A (weight fraction of Pb)	0.001(1000 ppm) 0.0009 (900 ppm) 0.0008 (800 ppm) 0.0006 (600ppm) 0.0004 (400 ppm) 0.0002 (200 ppm) 0.000 1 (100 ppm)
$(\mu / \rho)_{Pb, \lambda pri}$ (Mass-absorption coefficient of Pb: primary wavelength)	2.37 cm^2 / g
$(\mu / \rho)_{water, \lambda K}$ (Mass-absorption coefficient of water: analyte line)	0.1661 cm^2 / g
$(\mu / \rho)_{water, \lambda pri}$ (Mass-absorption coefficient of water: primary wavelength)	0.1356 cm^2 / g
$I_{o,\lambda pri}$ (intensity of Tc-99m)	3.534×10^7 counts / second
P_A	5.108×10^{-6}

Based on equation [3.16], the intensity of secondary spectral line emitted by the target sample, Pb is equal to:

$$I_K = P_A I_{0,\lambda pri} C_A \left\{ \frac{(\mu / \rho)_{A, \lambda pri}}{(\mu / \rho)_{m, \lambda pri} + (\mu / \rho)_{m, \lambda K}} \right\}$$

For Pb concentration of 1000 ppm,

$$I_K = P_A I_{0,\lambda pri} C_A \left\{ \frac{(\mu / \rho)_{A,\lambda pri}}{(\mu / \rho)_{m,\lambda pri} + (\mu / \rho)_{m,\lambda K}} \right\}$$

$$= (5.108 \times 10^{-6})(3.534 \times 10^{7})(0.001) \left\{ 7.855 \right\}$$

$$= 1.418 \text{ counts / second}$$

Using similar calculation the intensity of secondary spectral line for different lead concentrations are obtained as shown in table 5.7.

Table 5.7: The Intensity of secondary spectral line and counts within 400 seconds for each concentration of Pb (Theoretical Calculation)

Concentration (ppm)	Intensity (counts / second)	Counts (400 seconds)
1000	1.418	567.2
900	1.276	510.4
800	1.134	453.6
600	0.851	340.4
400	0.567	226.8
200	0.283	113.2
100	0.142	56.8

Table 5.8 shows the comparison of calculations in counts/second for the various concentrations with the experimental results. The higher intensity of experimental results has been noted. The theoretical calculation shows divergence if compared with the experimental results. This is due to the measurement of counts by Quantum MCA was based on the selected channel, namely ROI (Region of Interest) which had been set for the whole experiment to identify and determine the region total counts of Pb K-lines. However, for the theoretical model only the total counts at the peak of $K_{\alpha 1}$ of Pb is calculated instead. Unlike the experiment where the regional measurement is considered. The variation of 25.2% between the experimental and theoretical results for Pb concentration of 100 ppm, shows the low detection counts

for $K_{\alpha 1}$ even though the measurement counts is based on the ROI. Figure 5.6 shows the graph plotted in the intensity (counts/second) versus concentrations of Pb.

Table 5.8: The Comparison of Intensity of Theoretical and Experimental Results

Concentration (ppm)	Theoretical: Intensity (counts / second)	Experimental: Intensity (counts / second)	Variation in %
1000	1.418	3.315 ± 0.958	57.2
900	1.276	2.190 ± 0.958	41.7
800	1.134	2.165 ± 0.965	47.6
600	0.851	1.445 ± 0.965	41.1
400	0.567	1.323 ± 0.955	57.1
200	0.283	1.141 ± 0.930	75.2
100	0.142	0.190 ± 0.920	25.2

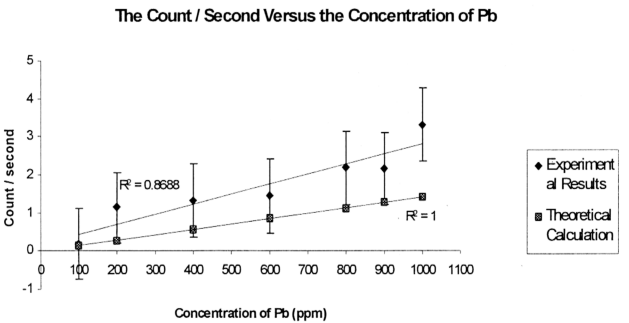

Figure 5.6: Intensity (Counts / second) versus Concentrations of Pb using theoretical calculation and experimental results

5.2.3 Assumptions in Theoretical Calculation

A few assumptions have been made in order to perform this theoretical model:

1. Homogeneous scattering of the excitation source and the second spectral line of the target sample, in the absence of multiple scatters.
2. The activity of Tc-99m although in the ranged of ~ 40 mCi to ~ 40.5 mCi, the value taken for this calculation is fixed at 40.3 mCi.
3. The detector efficiency is assumed to be 100%.

5.3 Conclusion

The simple detector system using the XR-100T detector and Tc-99m in this project is found not to be a suitable tool to detect Pb concentrations, which are lower than 800 ppm. The failure of the system to detect the peaks of XRF K-lines of Pb especially for the concentrations lower than 800 ppm had caused the high percentage errors in the calculation of average mean of differences for each concentration compared with the respective background measurements.

The use of Tc-99m as an excitation source with gamma energy of 140.5 keV, is far above the binding energy of K shell of Pb, resulting in the lower cross section for photoelectric interaction. Thus, the probability of photoelectric interaction is reduced. Since this interaction is dominant in X-ray fluorescence process, Cd-109, which has the gamma energy of 88.036 keV to the K shell of Pb, should be a more suitable excitation source to be used instead of Tc-99m. However due to its short half-life and high cost, it is not possible to employ them in this experiment.

A simple theoretical model has been formed to calculate the total count for the peak of Pb $K_{\alpha 1}$. This model is based on the secondary spectral-line intensity emitted by the analyte after excitation and de-excition of K level electrons of Pb. The calculation of counts has been used to compare and further confirmed the experimental results.

The theoretical calculation result was not in arrayed with the experimental result. This variation is because to the theoretical model being employed is based only on the calculation of counts for the $K_{\alpha 1}$ peak, while in the experimental setup the measurement of the (entire) range of channels is being considered.

References:

C.E.Webber, D.R. Chettle, C.L.Gordon and D.C.F. Muir, *An Improved Instrument for In Vivo Bone Lead Measurements using a 109Cd Point Source,* NIEHS X-ray Fluorescence Workshop, July 1992.

Chettle D.R., Scott M.C., Somervaille L.J., 1991, *"Lead in bone: sampling and quantitation using K X-rays excited by ^{109}Cd",* Environmental Health Perspectives 91, 49-55.

D.A.Bradley, Lynn Kissel and R.H.Pratt, 1999, *Elastic Photon Scattering and Normalization of In Vivo XRF Analyses of Lead in Bone,* X-RAY SPECTROM. 28, XRS363

E. P. Bertin, 1978, *Introduction to X-ray Spectrometric Analysis;* Plenum Press: New York and London, pg. 63

Green S., Bradley D.A., Palethorpe J.E., Mearman D., Chettle D.R., Lewis A., Mountford P.J., Morgan W.D., 1992, *"An enhanced-sensitivity K shell XRF technique for tibial-Pb determination",* Physics in Medicine and Biology.

K.Debertin and R.G.Helmer, 1988, *Gamma-and X-ray Spectrometry with Semiconductor Detectors,* North-Holland, pg. 31-35, 348.

P.Bloch, G.Garavaglia and G.Mitchell and I.M.Shapiro, (1976), *Measurement of Lead Content of Children's Teeth in situ by X-ray Fluorescence*, Phys.Med.Biol., vol.20, no.6, 56-63.